Bending Elastic Moduli of the Surfactant Film and Properties of a Winsor II Microemulsion System

Willem K. Kegel,*,† Igor Bodnàr, and Henk N. W. Lekkerkerker

Van't Hoff Laboratory, University of Utrecht, Padualaan 8, 3584 CH Utrecht, The Netherlands

Received: July 13, 1994; In Final Form: October 12, 1994[⊗]

The bending elastic modulus K and the Gaussian bending elastic modulus $\bar{K}$ of the surfactant film in a microemulsion system composed of sodium dodecyl sulfate (SDS), cyclohexane, water plus salt and two different cosurfactants, pentanol and hexanol, are presented. K is deduced from ellipsometry at the planar surfactant film at the macroscopic oil−brine interface, while $\bar{K}$ is obtained from properties of Winsor II microemulsion equilibria. These properties involve the volume fraction dependence of the (mean) droplet size, polydispersity of the droplet radius and interfacial tensions between the planar microemulsion−brine interface. The values of the bending elastic moduli are compared with the global phase behavior of these systems as reported recently (Kegel, W. K.; Lekkerkerker, H. N. W. *J. Phys. Chem.* **1993**, *97*, 11124).

1. Introduction

In recent work[1,2] the phase behavior of a system composed of sodium dodecyl sulfate, brine (aqueous NaCl solution), cyclohexane, and a cosurfactant (pentanol or hexanol or mixtures thereof) was studied. Using equal volumes of water and oil phase, a dramatic difference in (global) phase behavior was observed upon replacing pentanol by hexanol as a cosurfactant. At relatively low surfactant concentration and increasing cosurfactant concentration, in the pentanol system the "classical" phase progression[3] Winsor I (oil droplets in water coexisting with an excess oil phase), Winsor III (a bicontinuous phase in equilibrium with excess oil and water), Winsor II (water droplets in oil coexisting with excess water) was observed. In the hexanol system, however, we observed the progression Winsor I, Winsor III, four-phase equilibrium water−lamellar phase−bicontinuous phase−oil, Winsor III, Winsor II. This behavior can be rationalized in terms of a competition between a lamellar and a bicontinuous phase. This competition in turn is governed by the bending elastic modulus K and the modulus of Gaussian curvature $\bar{K}$. From the experimental length scales observed in the bicontinuous microemulsion phases it can be concluded that K is of order $0.1k_BT$ larger in the system with hexanol as cosurfactant than in the system with pentanol as cosurfactant. From the phenomenological interfacial model for microemulsion phase behavior of Andelman et al.[4] it follows that this indeed provides a rational for the increased stability of the lamellar phase. A quantitative comparison between theory and experiment reveals the necessity to include the variation of $\bar{K}$ with cosurfactant chain length as well.

In this paper we investigate the effect of the change of the cosurfactant chain length on the bending elastic moduli and the properties of Winsor II microemulsions. The bending elastic modulus K is determined by studying the flat oil−brine interface covered with a (mixed) surfactant layer using the ellipsometry technique.[5] The modulus of Gaussian curvature $\bar{K}$ is coupled to the topology of a surface and can therefore in principle be determined only in systems in which this topology is variable. This can be realized in droplet type microemulsions coexisting with an excess phase. In these systems the topology can be changed by a variation in the number of droplets which can be produced by a variation in the amount of surfactant in the system. From the dependence of the mean droplet radius, droplet size polydispersity, and the interfacial tension between the microemulsion and the excess phase on the total volume fraction of the droplets one can obtain information about K and $\bar{K}$.

In the next section we present a thermodynamic treatment of Winsor II microemulsion systems that is based upon a theory first presented by Overbeek.[6] This theory is combined with a phenomenological expression for the curvature free energy given by Helfrich.[7] From this treatment an expression is obtained for the droplet size distribution as a function of $(2K + \bar{K})$, $2K/R_0$, and γ with R_0 the preferred radius of curvature and γ the interfacial tension of the planar interface between the microemulsion and brine. In section 3 we present details of sample preparation and the background of the experimental techniques used in this work (ellipsometry, small-angle X-ray scattering). In section 4 we present the results and show how the bending elastic moduli K and $\bar{K}$ can be obtained separately by combining the results of the various techniques. The results are discussed in section 5 where we also discuss the values of the bending elastic moduli in relation with the observed phase behavior.

2. Theory of Winsor II Microemulsion Systems

In a microemulsion system, the size of the domains of the dispersed phase is in general determined by the area/volume ratio of the system, expressed by the surfactant concentration. Experimentally, a lower limit for this ratio is found. As soon as the surfactant concentration falls below a certain value, a phase separation into a microemulsion and an excess liquid phase occurs. The total droplet area of these systems is determined by the amount of surfactant but the system is free to choose the dispersed volume and hence the (mean) droplet radius. Here we concentrate on water-in-oil microemulsions coexisting with excess water, referred to as Winsor II systems.

The size distribution of thermodynamically stable emulsions was studied as early as 1927 by Volmer[8] using a kinetic mass action model. He obtained for the distribution function for the

† Present address: Department of Chemistry and Biochemistry, University of California, Los Angeles, 405 Hilgard Avenue, Los Angeles, CA 90024-1569.

* To whom all correspondence should be addressed.

⊗ Abstract published in *Advance ACS Abstracts,* February 15, 1995.

0022-3654/95/2099-3272$09.00/0

number of disperse-phase drops

$$P(R) = \text{constant} \cdot R^m \exp(-(4\pi R^2\sigma)/k_B T) \quad (1)$$

where R is the droplet radius, σ is the interfacial tension between the dispersed droplets and the continuous phase, k_B is Boltzmann's constant, and T is the absolute temperature. The value of the exponent m depends sensitively on the model in the derivation of (1). In his early publications[8a] Volmer found $m = 2$, whereas in a later one[8b] using the correction to the Gibbs–Kelvin equation discovered by Kuhrt[9] he obtained a value for m as high as 14.

In the last few years several thermodynamic treatments for the polydispersity in microemulsions have appeared.[6,10,11] These treatments are all based upon the multiple chemical equilibrium approach as embodied in the law of mass action. They differ in details about the relative importance of various contributions to the relevant Gibbs free energy and therefore the final results differ. However they share the common feature that the polydispersity is determined by γ, $(2K + \bar{K})$, and $2K/R_0$.

Here we describe a somewhat simplified version of a thermodynamic theory of polydisperse droplet type microemulsions as presented by Overbeek.[6] This theory is combined with a phenomenological expression of the curvature free energy given by Helfrich.[7] From this combination, size distributions are obtained and (implicitly) the volume fraction dependence of the (mean) droplet radius. We consider (spherical) droplets composed of water and salt, covered with a surfactant monolayer. We neglect the solubility of surfactant in the water-and-oil phases and the thickness of the monolayer. These assumptions seem reasonable for "strong" amphiphiles (i.e., surfactants with a strong affinity for the oil–water interface) and droplets that are large compared to the surfactant monolayer thickness.

The Gibbs free energy of the droplet type microemulsion system can be written as

$$G = \sum_i N_i \mu_i = \sum_i N_{im} \mu_i + \sum_j N_{dj} \mu_{dj} \quad (2)$$

where N_{im} are the amounts of components i in the continuous medium and N_{dj} and μ_{dj} are the number of droplets of category j and their chemical potential. We shall specify j later. All droplet categories have different radii, volumes, areas, etc. Since the pressure inside the droplets is expected to be different from the ambient pressure p, we first give the Helmholz free energy

$$F = \sum_i N_{im}\lambda_{im} + \sum_i \sum_j N_{ij}\lambda_{ij} - pV_m - \sum_j (p + \Delta p_j)V_{dj} + \sum_j \sigma_j A_j + F_{mix} \quad (3)$$

with λ_{im} and λ_{ij} the chemical potentials of component i in the continuous medium and in the droplets of category j when they are considered separately.[12] N_{ij} is the amount of i in the droplets of type j, V_{dj} and A_j are the total volume and area of droplets of category j, Δp_j is the pressure difference between the droplets of category j and the continuous medium, and σ_j is the interfacial tension of droplets j. The Gibbs free energy

$$G = F + pV = \sum_i N_{im}\lambda_{im} + \sum_i \sum_j N_{ij}\lambda_{ij} - \sum_j \Delta p_j V_{dj} + \sum_j \sigma_j A_j + G_{mix} \quad (4)$$

with V the total volume. We eliminate Δp_j by using the generalized Laplace equation[13]

$$\Delta p_j = \frac{2\sigma_j}{R_j} - \frac{2c_j}{R_j^2} \quad (5)$$

where R_j denotes the radius of droplets of type j and c_j is the bending moment

$$c_j = (\partial\sigma/\partial(2/R))_{R=R_j} \quad (6)$$

which will be related to the bending elastic moduli of the droplet interface later.

It is convenient to express A_j and V_{dj} in R_j and N_{dj}:

$$A_j = N_{dj} 4\pi R_j^2 \quad (7)$$

$$V_{dj} = N_{dj} \cdot {}^4/_3 \pi R_j^3 \quad (8)$$

The free energy of mixing reads, for low droplet concentrations

$$F_{mix} = G_{mix} = k_B T \sum_j N_{dj} f(\phi_j, R_j) \quad (9)$$

with

$$f(\phi_j, R_j) = \ln \phi_j - 1 - {}^3/_2 \ln(16R_j^3/\bar{v}_w) \quad (10)$$

where $\bar{v}_w$ denotes the molecular volume of water, and

$$\phi_j = {}^4/_3 \pi N_{dj} R_j^3 / V \quad (11)$$

In Appendix A a simple derivation of G_{mix} is given. The first two terms in eq 10 are based upon (ideal) mixing of hard spheres in a solvent and the last term accounts for the translational fluctuations of the center of mass of a fixed droplet.[14] Combining eqs 5–11, eq 4 becomes

$$G = \sum_i N_{im}\lambda_{im} + \sum_i \sum_j N_{ij}\lambda_{ij} + \sum_j {}^4/_3 \pi R_j^2 N_{dj}\left(\sigma_j + \frac{2c_j}{R_j}\right) + k_B T \sum_j N_{dj} f(\phi_j, R_j) \quad (12)$$

For the components in the continuous medium we find

$$\mu_i = \left(\frac{\partial G}{\partial N_{im}}\right)_{T,p,N_{jm\neq im}} = \lambda_{im} - k_B T \frac{\sum_j N_{dj}}{V} \bar{v}_i \quad (13)$$

thus

$$\sum_i N_{im}\mu_i = \sum_i N_{im}\lambda_i - k_B T \sum_j N_{dj} \quad (14)$$

where we have dropped a term linear in ϕ. The reason is that as soon as droplet interactions are not neglected, other terms also proportional to ϕ will appear. From eqs 9–12 and 14 we have

$$\mu_{dj} = \sum_i \frac{N_{ij}\lambda_{ij}}{N_{dj}} + {}^4/_3 \pi R_j^2 \left(\sigma_j + \frac{2c_j}{R_j}\right) + k_B T(\ln \phi_j - {}^3/_2 \ln(16R_j^3/\bar{v}_w)) \quad (15)$$

The λ's of the droplet components are related to the chemical

potentials:

$$\lambda_{ij} = \mu'_i + \int_p^{p+\Delta p_j} (\partial\lambda_i/\partial p)\, dp = \mu'_i + \Delta p_j \bar{v}_i = \mu'_i + \left(\frac{2\sigma_j}{R_j} - \frac{2c_j}{R_j^2}\right)\bar{v}_i \quad (16)$$

where μ'_i are the chemical potentials of the droplet components at ambient pressure p. In a microemulsion coexisting with an excess phase of the same composition as the droplets we have for the droplet components[6,12]

$$\mu'_i = \mu_i \quad (17)$$

Substituting eq 16 with 17 into eq 15, using

$$\sum_i \frac{N_{ij}}{N_{dj}} \bar{v}_i = {}^4/_3 \pi R_j^3 \quad (18)$$

for the water components, and writing μ_{dj} as the sum of the chemical potentials of the constituent molecular components, known as the law of mass action:

$$\mu_{dj} = \sum_i \frac{N_{ij}}{N_{dj}} \mu_i \quad (19)$$

we arrive at the size distribution:

$$\ln \phi_j = {}^3/_2 \ln(16 R_j^3/\bar{v}_w) - \frac{4\pi R_j^2 \sigma_j}{k_B T} \quad (20)$$

First of all we note the remarkable agreement (at least for the last term) with the size distribution already obtained by Volmer in 1927,[8] eq 1.

The first term at the right-hand side of eq 20 promotes large droplets (their volume fraction increases with $R^{9/2}$). The second term is the surface free energy of the system. If σ_j were no function of the curvature, the increase of the droplet size due to the first term would be offset by the increasingly more negative second term. Therefore, even in the absence of curvature effects, we find via this approach (at least in principle) a size distribution. However, several other features such as the dependence of the average size of the droplets on the total volume fraction can, in our view, be explained only by a curvature dependence of the interfacial tension. Therefore we now relate σ_j to the bending elastic moduli and the preferred curvature of the droplet interface.

For a sphere of radius R the curvature free energy in the harmonic approximation is given by

$$F_c = \int \left[2K\left(\frac{1}{R} - \frac{1}{R_0}\right)^2 + \frac{\bar{K}}{R^2}\right] dA \quad (21)$$

with K (as already mentioned) the bending elastic modulus, $\bar{K}$ the modulus associated with Gaussian curvature, and R_0 the preferred radius of curvature. The interfacial tension of the droplet interface is

$$\sigma_j = \gamma + \int_0^{2/R_j} \left(\frac{\partial\sigma}{\partial(2/R)}\right) d(2/R) \quad (22)$$

$\gamma \equiv \sigma(R \to \infty)$ is (in this model) the interfacial tension between the microemulsion and the excess phase. Since

$$\left(\frac{\partial\sigma}{\partial(2/R)}\right) = c = \left(\frac{\partial^2 F_c}{\partial A\, \partial(2/R)}\right) = \frac{1}{R}(2K + \bar{K}) - \frac{2K}{R_0} \quad (23)$$

we find

$$\sigma_j = \gamma + \frac{(2K + \bar{K})}{R_j^2} - \frac{4K}{R_0 R_j} \quad (24)$$

so that the category distribution becomes

$$\ln \phi_j = {}^3/_2 \ln \frac{16 R_j^3}{\bar{v}_w} - \frac{4\pi}{k_B T}\left\{(2K + \bar{K}) - \frac{4K R_j}{R_0} + R_j^2 \gamma\right\} \quad (25)$$

Taking into account size (and no shape) fluctuations only, a natural choice for the droplet categories j is the number of surfactant molecules per droplet or

$$j = 4\pi R_j^2/\sigma_s \quad (26)$$

with σ_s the area occupied by a surfactant molecule.

3. Experimental Section

Materials. Sodium dodecyl sulfate (SDS) was specially pure grade from BDH. Cyclohexane, 1-pentanol, 1-hexanol, and NaCl were Baker analyzed reagents. Deionized water was doubly distilled before use.

Sample Preparation. The samples were prepared by carefully pouring equal volumes of initial oil phase on initial water phase. Three kinds of sample series were studied, subsequently denoted as I, II, and III. The initial water phases for the samples used for ellipsometry (series I) consisted of various concentrations of NaCl and 0.07% (w/w) SDS being of order 10 times the critical micelle concentration.[15] The oil phase was composed of 15% (w/w) pentanol or 8% (w/w) hexanol in cyclohexane.

For the Winsor II equilibria (series II), the water phase was composed of 0.20 M NaCl and various amounts of SDS. The oil phase consisted of cyclohexane and various amounts of pentanol or hexanol. Equilibrium was attained by gently rolling the samples on a roller bench for several days. Subsequently the samples were permitted to equilibrate at constant temperature ((25 ± 0.1) °C). The amount of alcohol in the oil phase was corrected for the uptake in the SDS–alcohol monolayer at the cyclohexane–brine interface. This correction was determined from dilution titrations.[16] In the pentanol system 3.12 additional alcohol molecules and in the hexanol system 1.77 additional alcohol molecules per SDS molecule were added. Apparently the cosurfactant/surfactant ratios in the curved monolayer are different from the ones in the planar monolayer.[15] This was also observed by van Aken[17] who showed (using synchrotron SAXS) that the molecular area of SDS in the droplet interface remains equal to the one in the planar interface. The "free" cosurfactant concentrations (i.e., the concentration without SDS) were chosen such as to obtain a mean droplet radius of approximately 15 nm corresponding to 18.2% (w/w) pentanol and 8.8 (w/w) hexanol initially in the oil phase.

We also used data from measurements on Winsor II systems described in ref 17. These series are referred to as sample series III.

Ellipsometry. The use of ellipsometry to determine the bending elastic modulus of a surfactant monolayer at the (planar) oil–brine interface was first presented by Meunier.[5] We summarize the method below.

Ellipsometry allows us to measure the polarization state of light reflected from an interface between two materials.[18] This polarization state is determined by properties of the dielectric constant profile being composed of a structural variation and a fluctuation contribution caused by thermal corrugations of the interface. The polarization state is defined by

$$r = r_p/r_s = \varrho e^{i\Delta} \tag{27}$$

where r denotes the (complex) ellipsometric coefficient and r_p and r_s are the reflectivity amplitudes of the electric field for p (parallel to the plane of incidence) and s (perpendicular) polarized light. $\Delta = \delta_p - \delta_s$ with δ_p (δ_s) the phase shift experienced upon reflection of light polarized parallel (perpendicular) to the plane of incidence. Δ and ϱ can be measured separately by ellipsometry. The Brewster angle θ_B is defined as $\Delta(\theta_B) = \pi/2$. At this angle, there is a general relation between η, which depends upon interfacial properties, and ϱ[19]

$$\eta = \frac{\lambda}{\pi}\frac{n_1^2 - n_2^2}{(n_1^2 + n_2^2)^{1/2}}\varrho \tag{28}$$

with λ the wavelength of light and n_1 and n_2 the refractive indexes of the two phases. η is effectively the sum of a "structural" term η_s and a "roughness" term η_r

$$\eta = \eta_s + \eta_r \tag{29}$$

η_s is model dependent and will not be specified. The roughness term η_r is related to the mean-squared amplitude of surface corrugations which is obtained by a statistical analysis of the thermal modes. The final result is[5]

$$\eta_r = -\frac{3k_BT(n_1^2 - n_2^2)^2}{8(n_1^2 + n_2^2)}(\gamma K)^{-1/2} \tag{30}$$

In a microemulsion system one may vary γ by, e.g., varying the salt concentration. It is expected that this does not significantly influences K as long as the salt concentration is not too low and the range over which it is varied is not too broad.[20] By plotting η obtained from ellipsometry (eq 28) against $\gamma^{-1/2}$, K is obtained from the slope and η_s from the intercept (eqs 29 and 30).

The home-built (polarization modulation) ellipsometer is based upon the design of Meunier,[21] who used the optical arrangement as reported by Jasperson and Schnatterly[22] and Beaglehole.[23] It is mounted vertically to reflect off the horizontal liquid−liquid interface. The interfacial tensions necessary for the interpretation of the results were measured with a spinning drop tensiometer (Krüss, Hamburg, SITE 04). The measurements were complicated by the formation of liquid crystals in the droplets. This effect could be avoided (though not in all cases) by very slowly introducing the less dense phase into the denser phase. All measurements were carried out at 25 °C.

Determination of the Droplet Radius from the Water Content and Small-Angle X-ray Scattering. The droplet radii in the Winsor II systems were determined from the water content in the oil phase using Karl−Fisher titrations and from small-angle X-ray scattering (SAXS). The total area in the system is known from the amount of SDS by $A = N_s\sigma_s$ with N_s the number of surfactant molecules in the system corrected for the cmc.[15] The molecular area σ_s is known from interfacial tension measurements and application of the Gibbs adsorption equation: $\sigma_s = 0.94$ nm^2 for both the pentanol and hexanol system.[15] So from the water content, V_w, we obtain the radius:

$$R_w = 3V_w/A = \langle R^3\rangle/\langle R^2\rangle \tag{31}$$

SAXS measurements were made with an Anton Paar Kratky camera. The apparatus is described in more detail in ref 2.

In a dilute system of particles, the radius of gyration R_g is obtained from the scattered intensity $I(q)$ measured with SAXS at low scattering vector q:[24]

$$I(q\to 0) = I(q=0)\exp(-q^2R_g^2/3) \tag{32}$$

In case of a (dilute) polydisperse system of spherosymmetrical particles, the scattered intensity is the sum of the intensities scattered by all particle categories. The experimentally determined R_g is an average over all particles but it reflects a different moment of the size distribution compared to the radius R_w. As shown, e.g., by Moonen et al.[25] for homogeneous particles:

$$R_g^2 = {}^3/_5\frac{\langle R^8\rangle}{\langle R^6\rangle} \tag{33}$$

The microemulsion droplets studied here are not homogeneous but contain a layer of surfactant molecules. Because of the high electron density of the sulfate groups, these shells contribute significantly to the scattered intensity. In Appendix B we derive R_g of a polydisperse ensemble of particles with a shell. The result is

$$R_g^2 = {}^3/_5([(\varrho_1 - \varrho_2)^2\langle R_1^8\rangle + (\varrho_1 - \varrho_2)(\varrho_2 - \varrho_s)(\langle R_1^3R_2^5\rangle + \langle R_1^5R_2^3\rangle) + (\varrho_2 - \varrho_s)^2\langle R_2^8\rangle]/[(\varrho_1 - \varrho_2)^2\langle R_1^6\rangle + 2(\varrho_1 - \varrho_2)(\varrho_2 - \varrho_s)\langle R_1^3R_2^3\rangle + (\varrho_2 - \varrho_s)^2\langle R_2^6\rangle]) \tag{34}$$

where R_1 and R_2 are the radii of the water core and the water core plus coated layer and ϱ_1, ϱ_2, and ϱ_s are the electron densities of the inner (water) core, the surfactant layer and the solvent. The electron densities are calculated from the densities of the constituting molecules in the liquid state and their number of electrons. It is assumed that the electron densities of the hydrocarbon tails of the adsorbed SDS and cosurfactant molecules are not significantly different from the electron density of the oil phase. The electron density ϱ_2 of the polar part of the surfactant shell is determined by the molecular area of SDS σ_s and by the shell thickness $d = R_2 - R_1$ via

$$\varrho_2 = \frac{N_e/\sigma_s}{d} + \varrho_1 \tag{35}$$

where N_e denotes the number of excess electrons of a sulfate group relative to the number of electrons of water. Equation 35 implies that increasing d is analogous to diluting the outer layer with water phase. The contribution of the cosurfactant adsorption to the electron density is neglected as in the model used, space is filled with water having about the same electron density as a hydroxy group. Fortunately, performing model calculations it turns out that R_g (and even the full form factor) is hardly affected when d is varied between 0.1 and 1.0 nm (and conservation of matter is taken into account by decreasing R_1 upon increasing d).

4. Results

4.1. Ellipsometry (Sample Series I). In Figure 1 the interfacial tensions as a function of the salt concentration are presented. The salt concentration ranges where excess oil and water phase are present are indicated by bars.

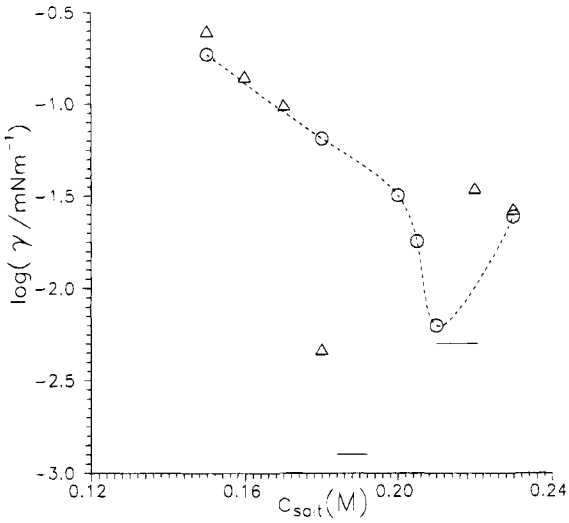

Figure 1. Interfacial tensions between water and oil phase as a function of the salt concentration of the pentanol system (circles) and the hexanol system (triangles). The three-phase (brine−microemulsion−oil) regions are indicated by the bars. The (dashed) line is a guide to the eye. Measurements were performed on sample series I (see text).

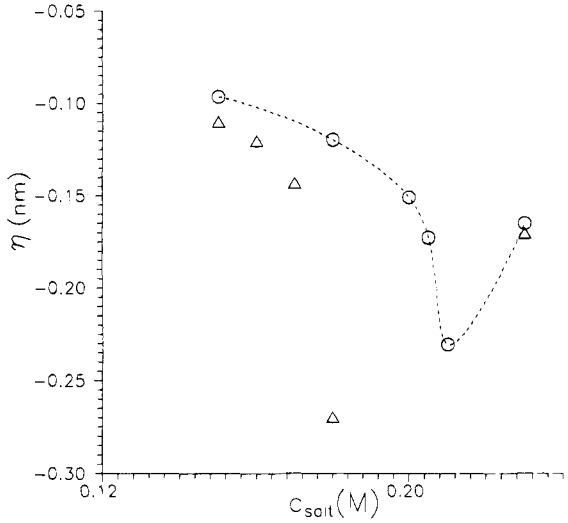

Figure 2. Ellipsometric coefficient η as a function of the salt concentration. Symbols the same as in Figure 1. (Sample series I, see text).

Figure 2 shows the ellipsometric coefficient η (calculated from the measured ϱ with eq (28) as a function of the salt concentration and in Figure 3 we plotted η against $(n_1^2 - n_2^2)/[(n_1^2 + n_2^2)\gamma^{1/2}]$. The slope of the lines give K being $(0.9 \pm 0.1)k_BT$ for the pentanol system and $(1.1 \pm 0.1)k_BT$ for the hexanol system.

4.2. Winsor II Microemulsion Systems. Unless stated otherwise, all measurements described below are performed on sample series II.

Average droplet radii as well as volume fractions are obtained from the water content (Karl−Fisher titration) and the (droplet) area in the system using values of the molecular area of SDS and the critical micelle concentration as reported in ref 15.

The SAXS measurements were performed using a Cu tube as an X-ray source. As a consequence the scattered intensity was too low to permit a reliable determination of the radius of gyration below droplet volume fractions of about 0.02. Consequently the volume fraction dependence of the droplet radius as observed with SAXS is hardly significant.

We used a numerical procedure to "fit" the experimental R_w, ϕ data to eq 25. In principle, every datapoint fixes the total

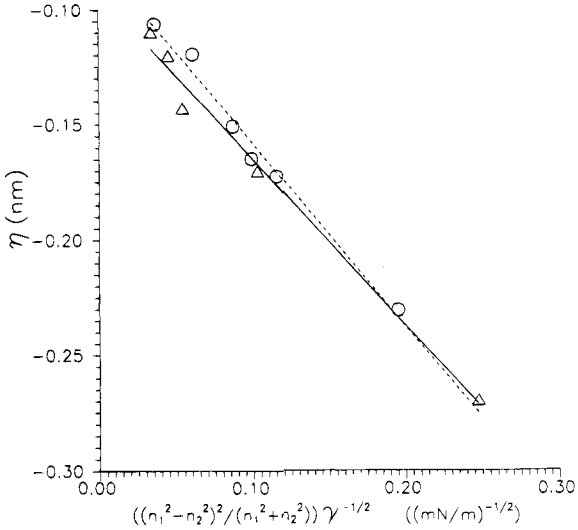

Figure 3. Ellipsometric Coefficient η as a Function of $(n_1^2 - n_2^2)/[n_1^2 + n_2^2)\gamma^{1/2}]$. Symbols the same as in Figure 1. The lines (dashed for pentanol and solid for hexanol systems) are linear best-fit lines. (Sample series I, see text).

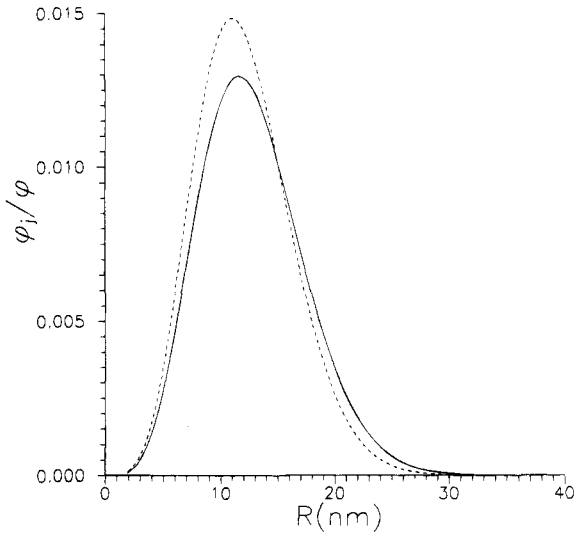

Figure 4. Calculated size distributions (eq 25) ϕ_j/ϕ versus R at $\phi = 0.025$ for the pentanol system (solid line) and the hexanol system (dashed line). Values of γ of 0.00244 mN/m (pentanol) and 0.00315 mN/m (hexanol) were used. The values of the other parameters ($(2K + \bar{K})$ and $2K/R_0$ are listed in Table 1.

volume fraction $\phi = \Sigma\phi_j$ and the radius obtained from the water titration $R_w = \langle R^3\rangle/\langle R^2\rangle$. For a single data point, the size distribution corresponding to these values is not unique, i.e., several values of $(2K + \bar{K})$, $(2K/R_0)$, and γ can be found that lead to the same values for R_w and ϕ. Fixed and unique values of $(2K + \bar{K})$ and $(2K/R_0)$ are found using a numerical procedure that takes into account the whole range of experimental R_w, ϕ data points. Typical size distributions for the pentanol and the hexanol systems are shown in Figure 4. The results for the whole experimental series of R_w, ϕ datapoints are depicted in Figures 5a (pentanol) and 6a (hexanol). With the fixed values of $(2K + \bar{K})$ and $(2K/R_0)$, γ is varied as shown in Figures 5b (pentanol) and 6b (hexanol). In Table 1 the values of $(2K + \bar{K})$ and $(2K/R_0)$ are listed together with a few polydispersities. These are calculated via

$$\epsilon^2 = \frac{\langle R^2\rangle - \langle R\rangle^2}{\langle R\rangle^2} \tag{36}$$

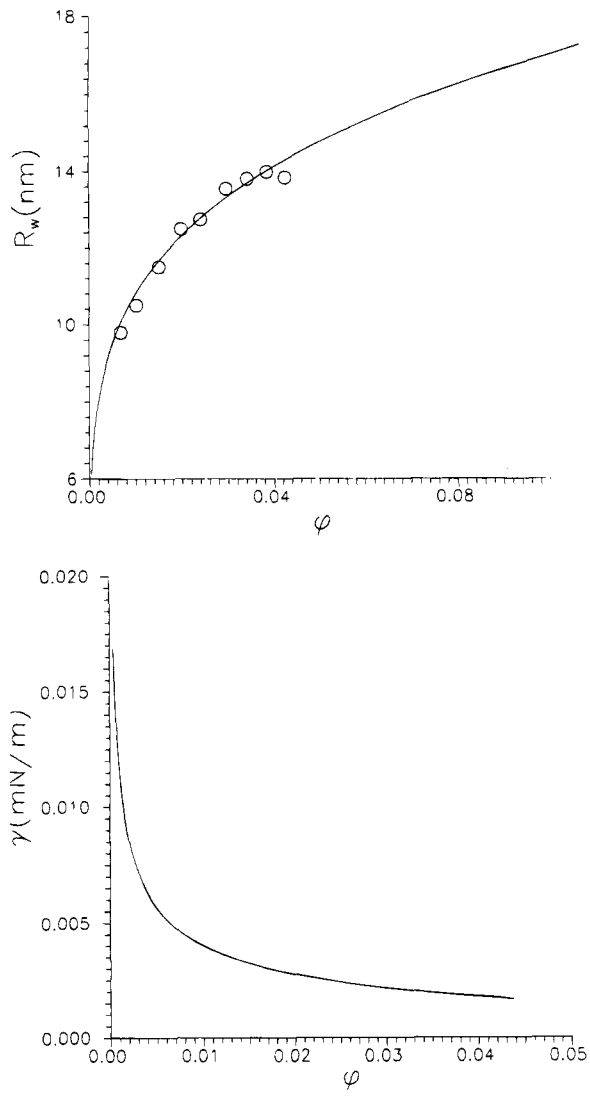

Figure 5. Experimentally determined droplet radius R_w for the pentanol system obtained from the water content of the microemulsion phase as a function of the droplet volume fraction. Solid lines are "best-fit" lines to eq 25 (see text; a, top). γ is varied as shown in b, bottom. Measurements were done on sample series II (see text).

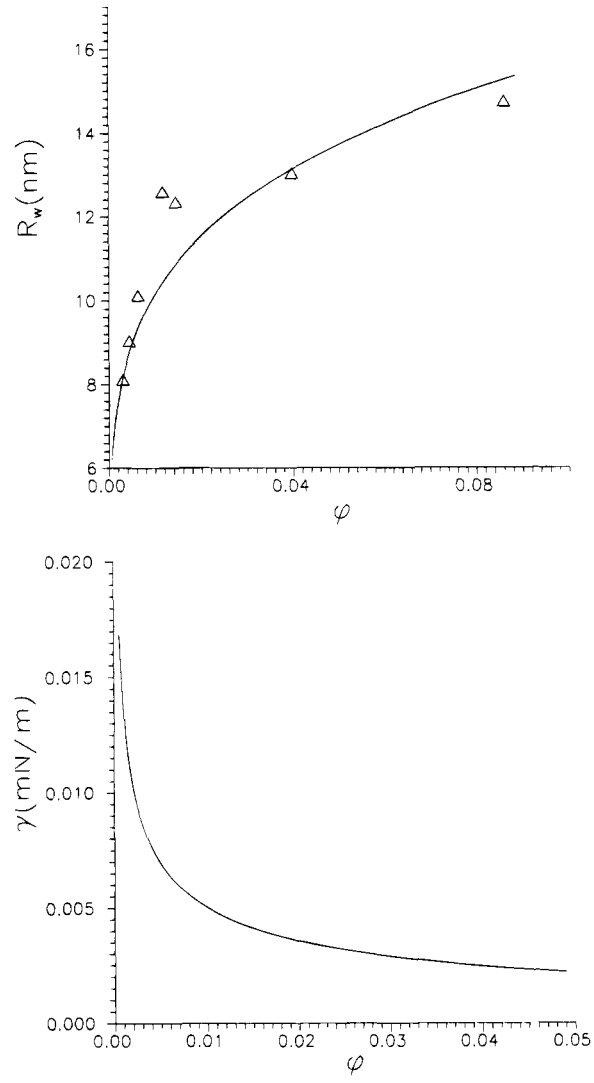

Figure 6. As Figure 5 but now for the hexanol system.

TABLE 1: Values of $(2K + \bar{K})$, $2K/R_0$ from "Best Fits" to Eq 25[a]

system	$(2K + \bar{K})k_BT$	$2K/R_0(k_BT/\text{nm})$
pentanol	2.30 (2.25)	−0.087 (−0.0070)
hexanol	2.28 (2.24)	−0.0080 (−0.0090)

Φ	ϵ(pentanol)	ϵ(hexanol)
0.001	0.39	0.38
0.01	0.43	0.42
0.05	0.46	0.44

[a] The values between brackets are the ones used to calculate R_w and R_g as a function of ϕ (Figure 7). The polydispesity ϵ as a function of the volume fraction ϕ is also given. Data refer to sample series II (see text).

The (slightly) negative values of $(2K/R_0)$ are regarded as unphysical. We come back at this point in the discussion section.

The size distributions obtained in the way described above are tested by measuring effectively two different moments of the size distributions: the radius from water titrations, eq 31, and the radius of gyration, eq 34. The results are shown in Figure 7. The somewhat different values of R_w in Figure 7 are due to the fact that different series of samples were used (most probably, the mean radius is sensitive for extremely small variations in the cosurfactant concentration). This is probably also the reason why slightly different values of $(2K + \bar{K})$ and $(2K/R_0)$ had to be used. The results are shown in Table 1. From Figure 7 it follows that the agreement between theory and experiment is excellent for the pentanol system, but the polydispersity of the hexanol system is clearly somewhat underestimated. In fact, using the volume fraction dependence of the droplet radius as "input parameters", the theory predicts approximately the same polydispersities (see Table 1).

The final confrontation with experiments concerns the interfacial tension of the planar microemulsion−excess brine interface. This parameter has hitherto been treated as a "free" quantity. The ϕ, R_w, and interfacial tensions were taken from van Aken[17] (sample series III). From the volume fraction dependence of the droplet radius (Figure 8a) we obtained $(2K + \bar{K}) = 2.53k_BT$ and $(2K/R_0) = +0.03k_BT/\text{nm}$. These values are somewhat different from the values for the pentanol system studied here (Table 1). This might be due to the larger amount of pentanol as used in ref 17 (i.e., 0.20 w/w initial in cyclohexane). The larger pentanol concentration may also explain the significantly smaller average droplet size in the system mentioned above. Especially the positive value of $(2K/R_0)$ is understandable since the larger pentanol concentration tends to bend the interface in the water direction thus making

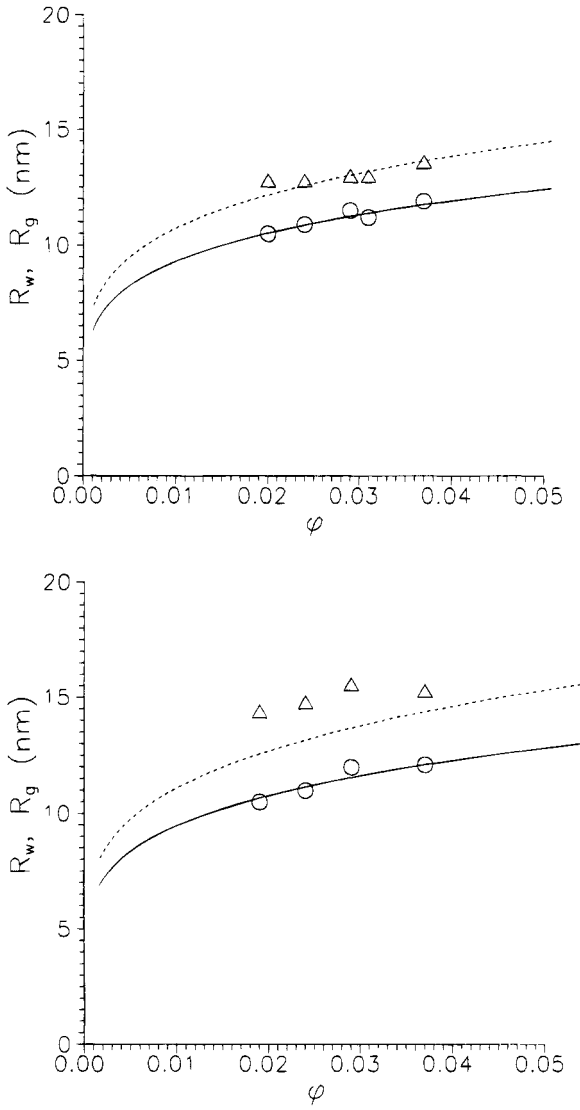

Figure 7. Experimental (points) and calculated (lines) R_w (circles and solid lines) and R_g (triangles and dashed lines) versus ϕ for the pentanol system (a, top) and the hexanol system (b, bottom). Experimental R_w and R_g are obtained from the water content and SAXS. The lines are calculated from the size distribution eq 25, see text. Sample series II under slightly different conditions as those in Figures 5 and 6 (see text).

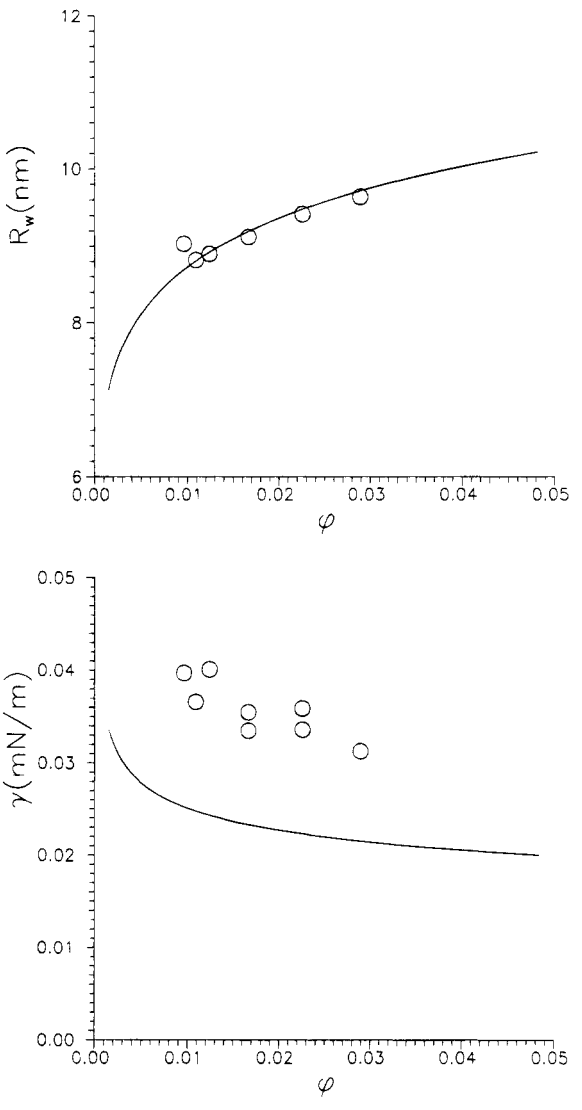

Figure 8. Data obtained from van Aken[14] (sample series III, see text). The droplet radius as a function of the volume fraction (a, top) and the interfacial tension as a function of the volume fraction (b, bottom). The solid line in b is follows from eq 25 after a "best-fit" to the datapoints in a (see text).

the spontaneous radius of curvature more positive. The variation of γ as a function of the droplet volume fraction necessary to produce the R_w, ϕ data is shown in Figure 8b, together with the experimental data from ref 17. The difference between theory and experiments is approximately 30%, but the theory qualitatively describes the dependence of γ on ϕ rather well.

5. Discussion and Conclusions

Before discussing the values of the bending elastic moduli of the systems studied here, we first make some remarks about the behavior of the Winsor II systems. From Figures 5 and 6 it follows that the (mean) droplet size in a Winsor II microemulsion system significantly depends upon the droplet volume fraction. This dependency can be fitted to eq 25. It is interpreted as a manifestation of the competition between mixing entropy (which tends to increase the number of droplets, thus decreasing their size) and curvature energy (preferring a constant radius). This can be shown more clearly from the result of a thermodynamic analysis of monodisperse systems[12,26]

$$R(\phi) = R_0\left(1 + \frac{\bar{K}}{2K} + \frac{k_B T}{8\pi K}(\ln \phi - {}^3/_2 \ln(16R^3/\bar{v}_w) + {}^3/_4)\right) \quad (37)$$

from which it follows that the droplet radius is indeed expected to increase with the volume fraction.

We tested the size distributions obtained from eq 25 by measuring effectively two different moments of the droplet radius (Figure 7). The agreement between theory and experiment is excellent for the pentanol system. In the case of the hexanol system, the calculated size distributions somewhat underestimates the real polydispersity. The underlying reason for this is not clear to us. It is however not considered as too serious as for still smaller polydispersities ($\epsilon < 0.30$), we found that the radii of gyration are already smaller than the radii obtained from the R_w's. Therefore we believe that the polydispersities obtained from "fitting" the theory to the volume fraction dependence of the droplet radius are in the correct range.

Although the theory describes the dependence of γ on the volume fraction (and R) qualitatively well (Figure 8), the quantitative agreement is considerably less satisfactory. We

TABLE 2: Values of the Bending Elastic Modulus K and the Gaussian Bending Elastic Modulus $\bar{K}$ for the Pentanol and the Hexanol System[a]

system	K/k_BT	$\bar{K}/k_BT$
pentanol	0.9	0.5
hexanol	1.1	0.08

[a] $\bar{K}$ is calculated from $(2K + \bar{K})$ obtained from the volume fraction dependence of the droplet radius (Table 1) and K obtained from ellipsometry. (Sample series II.)

note, however, that γ depends very sensitively on $(2K + \bar{K})$ and $(2K/R_0)$ and changes of a few percent in these parameters already gives a much better agreement. As is clear from a comparison of our results summarized in Table 1, even the use of different samples may give rise to such changes.

In Table 2 the values of K and $\bar{K}$ for the pentanol and the hexanol system are summarized. K increases with order a tenth of k_BT when hexanol instead of pentanol is used as a cosurfactant. This was already estimated from a length scale analysis in bicontinuous microemulsion systems composed of SDS, cyclohexane, brine and pentanol or hexanol.[2] We estimate the error in $\bar{K}$ as approximately $0.2k_BT$, so that we may conclude that $\bar{K}$ decreases with order $0.1k_BT$ when pentanol is replaced by hexanol as a cosurfactant. As shown by Helfrich,[27] $\bar{K}$ is the negative second moment of the lateral pressure profile $\Pi(z)$:

$$\bar{K} = -\int_{-\infty}^{+\infty} z^2 \Pi(z)\, dz \tag{38}$$

so that, since an increasing chain length causes an increased positive contribution to $\Pi(z)$, $\bar{K}$ is indeed expected to decrease with increasing cosurfactant chainlength. As pointed out in ref 1, $\Pi(z)$ is for the most part expected to be positive so that $\bar{K}$ will be negative. From the analysis presented here, however, positive values are found. This, together with the negative values of $2K/R_0$ (Table 1) casts some doubt on the free energy of mixing term eqs 9 with 10. It was found that a smaller absolute value of the term logarithmic in R gives rise to a positive $2K/R_0$ and negative $\bar{K}$, as it should. On the other hand, this term plays a crucial role in the droplet size distribution as without it (see eq 20), no (physical) size distribution is found at all. The problem concerning the free energy of mixing of microemulsion droplets is currently under study. We note that in a recent paper,[28] an approach similar in spirit but different in several important details from that used here was taken. They encountered the same problem concerning the determination of the absolute value of $\bar{K}$.

In an even more recent paper[29] values of $(2K + \bar{K})$ of the surfactant film in a Winsor II system made of AOT, water plus salt, and oil were presented. Both the chain length of the oil and the concentration of salt were varied. K was determined from ellipsometry, and a considerable variation of both K and $\bar{K}$ was observed. In this work, the experiments were conducted at a single (relatively high) salinity, and it is expected that variation of the salt concentration affects only the value of the Gaussian bending elastic modulus of a monolayer at relatively low salt concentrations.[20] It would be tempting to compare the values of $\bar{K}$ presented in ref 29 with those obtained for the systems studied here. However, the model used in ref 29 is rather different from the one used in this work, i.e., in ref 29 the systems are considered as monodisperse and their expression for the free energy of mixing is different from that used here. As mentioned above, the value of $\bar{K}$ one gets depends sensitively on the model used for the free energy of mixing. Therefore we may not compare the values of $\bar{K}$ presented in ref 29 with those obtained in this work.

It is nevertheless clear that upon increasing the cosurfactant chain length in the system studied here, K increases and $\bar{K}$ decreased with order $0.1k_BT$.

From eq 25 it follows that the polydispersity and the volume fraction dependence of the (mean) droplet radius depends upon two linear combinations of bending elastic quantities: $(2K + \bar{K})$ and $2K/R_0$. It can be seen from Table 1 that the variation of these quantities upon replacing pentanol for hexanol is only small. This is reflected in the observation that no dramatic difference in polydispersity and volume fraction dependence of the droplet radius are found in these systems. As mentioned in the introduction, in ref 2 a dramatic difference in the global phase behavior was found when pentanol is replaced by hexanol. It appears that the (bicontinuous) microemulsion phase is (relative to a lamellar phase) much less stable in the hexanol system compared to this phase in the pentanol system. Using a simple random mixing model, it was shown that the free energy of the microemulsion phase contains a term proportional to $(2K - \bar{K})$. From Table 2 it follows that this term increases considerably when pentanol is replaced by hexanol, which might explain the difference in stability of the microemulsion phase.

Acknowledgment. The authors gratefully acknowledge continuous enlightening discussions with Theo Overbeek about the work reported here. We thank Gerard Harder and Marco van Amerongen for skillfully constructing the ellipsometer, Carel van der Werf for doing the computer interfacing, and Jan Dhont for his useful suggestions during the construction of the ellipsometer. We are grateful to Jacques Meunier and Hamid Kellay for teaching W.K.K. the art of ellipsometry. Bob Aveyard is thanked for his kind permission to perform spinning drop measurements at the University of Hull, U.K. We thank Agnes Peels for performing preliminary work on volume fraction dependence of the droplet size. W.K.K. thanks Ger Koper for discussions and correspondence. Agienus Vrij, Gert-Jan Vroege, and Jan Dhont are thanked for their useful comments on the manuscript.

Appendix A. Calculation of the Free Energy of Mixing Droplets with a Solvent

In the following we present a very simple derivation of the free energy of mixing assuming ideal behavior of the droplets instead of using the Carnahan−Starling equation of state[12] being appropriate for the low volume fractions we are dealing with here. For clarity we assume a monodisperse system of droplets. The result is easily generalized to systems containing several droplet categories.

The free energy change G_{mix} of mixing droplets composed of (pseudo) component 2 with a solvent (component 1), is

$$G_{mix} = N_1(\mu_1 - \mu_1^\circ) + N_d(\mu_d - n_2\mu_2^\circ) \tag{A1}$$

with N_1 the number of solvent molecules, μ_1 the chemical potential of the solvent, μ_i° the standard chemical potential of component i, N_d the number of droplets, μ_d the chemical potential of a droplet, and n_2 the number of molecules of (pseudo) component 2 per droplet.

The relation between the chemical potential μ_1 and the osmotic pressure Π is

$$\mu_1 = \mu_1^\circ - \Pi\bar{v}_1 \tag{A2}$$

with $\bar{v}_1$ the molecular volume of the solvent. Π is model

dependent. As we are dealing with low volume fractions of droplets, we assume the ideal equation of state

$$\Pi = k_B T \varrho = k_B T N_d / V \tag{A3}$$

with ϱ the number density of the droplets. Again assuming ideal behavior, μ_d is

$$\mu_d = \mu_d^0 + k_B T \ln \phi \tag{A4}$$

where μ_d^0 is the standard chemical potential being different from $n_2\mu_2°$:

$$\mu_d^0 = n_2\mu_2° + \Psi \tag{A5}$$

According to the treatment of Reiss[14] the difference between μ_d^0 and $n_2\mu_2°$ can be attributed to the translational freedom of the center of mass of a fixed droplet. His analysis leads to[12]

$$\Psi = -\,{}^3/_2 \ln(16R^3/\bar{v}_w) \tag{A6}$$

with $\bar{v}_w$ the molecular volume of water. At low ϕ, $N_1\bar{v}_1/V \cong 1$ and thus

$$G_{mix} = k_B T N_d(\ln \phi - 1 - {}^3/_2 \ln(16R^3/\bar{v}_w)) \tag{A7}$$

This result is easily generalized to a system containing several droplet categories, leading to eqs 9 and 10.

There is no unanimity about the choice of Ψ in the literature. Several other choices are discussed in ref 12.

Appendix B. Calculation of the Guinier Radius of Gyration of an Ensemble of Polydisperse Particles with a Shell

At low scattering vector q the radius of gyration R_g for a single particle is conveniently defined by[24]

$$I(q\to 0)/(q=0) = \exp(-q^2R_g^2/3) \tag{B1}$$

with $I(q)$ the scattered intensity at scattering vector q. In dilute systems the normalized scattering intensity of an ensemble of particles is to a good approximation the sum of the intensities scattered by all particle categories:[30]

$$I(q) = \sum_i n_i B_i^2(q) \tag{B2}$$

where $B_i(q)$ denotes the scattering amplitude of a particle of category i and n_i the number of particles i per unit volume. Now n_i is just the probability to find a particle of category i, p_i, times the number of all particles per unit volume n:

$$n_i = p_i n \tag{B3}$$

We assume that the particles i differ only in their radius R so $p_i = p(R_i)$. The scattering amplitude is given by[30]

$$B_i(q) = \int_{\text{particle } i} d^3r\, [\varrho(\mathbf{r}) - \varrho_s] e^{i\mathbf{q}\cdot\mathbf{r}} \tag{B4}$$

the difference $\varrho(\mathbf{r}) - \varrho_s$ is the local contrast with respect to the solvent. For a spherosymmetrical ensemble of particles with a single shell of thickness $R_{2,i} - R_{1,i}$ with R_1 the radius of the inner core and R_2 the radius of the whole particle it follows from eqs B4 and B2

$$I(q=0) = (16\pi^2 n/9)\,((\varrho_1 - \varrho_2)^2\langle R_1^6\rangle + 2(\varrho_1 - \varrho_2)(\varrho_2 - \varrho_s)\langle R_1^3 R_2^3\rangle + (\varrho_2 - \varrho_s)^2\langle R_2^6\rangle) \tag{B5}$$

with ϱ_1 and ϱ_2 the scattering density of the inner core and the outer layer and

$$\langle R^n\rangle = \sum_i p(R_i) R_i^n \tag{B6}$$

At finite q we can write

$$I(q) = n\sum_i p(R_i)[4\pi((\varrho_1 - \varrho_2) f(q,R_{1,i}) + (\varrho_2 - \varrho_s) f(q,R_{2,i}))]^2 \tag{B7}$$

with

$$f(q,R) = [\sin(qR) - qR\cos(qR)]/q^3 \tag{B8}$$

at small q, more precisely when $qR < 1$ we may expand eq B8:

$$f(qR<1,R) = {}^1/_3\left(R^3 - \frac{1}{10}q^2R^5\right) \tag{B9}$$

substituting eqs B9 into B7 and using B5 we get, after some algebra

$$I(q\to 0)/I(q=0) = 1 - (q^2/5)([(\varrho_1 - \varrho_2)^2\langle R_1^8\rangle + (\varrho_1 - \varrho_2)(\varrho_2 - \varrho_s)(\langle R_1^3 R_2^5\rangle + \langle R_1^5 R_2^3\rangle) + (\varrho_2 - \varrho_s)^2\langle R_2^8\rangle]/[(\varrho_1 - \varrho_2)^2\langle R_1^6\rangle + 2(\varrho_1 - \varrho_2)(\varrho_2 - \varrho_s)\langle R_1^3 R_2^3\rangle + (\varrho_2 - \varrho_s)^2\langle R_2^6\rangle]) + \ldots \tag{B10}$$

Comparing eqs B10 and B11 (and recognizing the Taylor expansion of the exponent) gives

$$R_g^2 = {}^3/_5([(\varrho_1 - \varrho_2)^2\langle R_1^8\rangle + (\varrho_1 - \varrho_2)(\varrho_2 - \varrho_s)(\langle R_1^3 R_2^5\rangle + \langle R_1^5 R_2^3\rangle) + (\varrho_2 - \varrho_s)^2\langle R_2^8\rangle]/[(\varrho_1 - \varrho_2)^2\langle R_1^6\rangle + 2(\varrho_1 - \varrho_2)(\varrho_2 - \varrho_s)\langle R_1^3 R_2^3\rangle + (\varrho_2 - \varrho_s)^2\langle R_2^6\rangle]) \tag{B11}$$

being the radius of gyration of an ensemble of polydisperse particles with a shell.

References and Notes

(1) Kegel, W. K.; Lekkerkerker, H. N. W. *Colloids Surfaces* **1993**, *A76*, 241.
(2) Kegel, W. K.; Lekkerkerker, H. N. W. *J. Phys. Chem.* **1993**, *97*, 11124.
(3) Winsor, P. A. *Trans. Faraday Soc.* **1948**, *44*, 376.
(4) Andelman, D.; Cates, M. E.; Roux, D.; Safran, S. A. *J. Chem. Phys.* **1987**, *87*, 7229.
(5) Meunier, J. *J. Phys. Lett. (Fr.)* **1985**, *46*, L-1005. Meunier, J. *J. Phys. (Fr.)* **1987**, *48*, 1819.
(6) Overbeek, J. Th. G. *Prog. Colloid Polym. Sci.* **1990**, *83*, 1. Overbeek, J. Th. G. In *Surfactants in solution*; Vol. 11, Mittal, K. L., Shah, D. O., Eds.; Plenum Press: New York, 1991; p 3.
(7) Helfrich, W. *Z. Naturforsch.* **1973**, *C28*, 693.
(8) (a) Volmer, M. *Z. Phys. Chem.* **1927**, *125*, 151. (b) Volmer, M. *Z. Phys. Chem.* **1957**, *206*, 181.
(9) Kuhrt, F. *Z. Phys.* **1952**, *131*, 185.
(10) Borcovic, M.; Eicke, H.-F.; Ricka, J. *J. Colloid Interface Sci.* **1989**, *131*, 366. Borcovic, M. *J. Chem. Phys.* **1989**, *91*, 6268.
(11) Eriksson, J. C.; Ljunggren, S. *Prog. Colloid Polym. Sci.* **1990**, *81*, *41*.
(12) Overbeek, J. Th. G.; Verhoeckx, G. J.; de Bruyn, P. L.; Lekkerkerker, H. N. W. *J. Colloid Interface Sci.* **1987**, *119*, 422.

(13) Rowlinson, J. S.; Widom, B. *Molecular theory of capillarity*; Oxford: New York, 1989.
(14) Reiss, H. *J. Colloid Interface Sci.* **1975**, *53*, 61.
(15) Kegel, W. K.; van Aken, G. A.; Bouts, M. N.; Lekkerkerker, H. N. W.; Overbeek, J. Th. G.; de Bruyn, P. L. *Langmuir* **1993**, *8*, 152.
(16) Verhoeckx, G. J.; de Bruyn, P. L.; Overbeek, J. Th. G. *J. Colloid Interface Sci.* **1987**, *119*, 409.
(17) van Aken, G. A. *Thesis* Rijksuniversiteit Utrecht, 1990.
(18) Azzam, R. M. A.; Bashara, N. M. *Ellipsometry and polarized light*; Amsterdam, 1977.
(19) Drude, P. *The Theory of Optics*; Dover: New York, 1959.
(20) Lekkerkerker, H. N. W. *Physica* **1989**, *A159*, 319.
(21) Meunier, J., personal communications.
(22) Jasperson, S. N.; Schnatterly, S. E. *Rev. Sci. Instrum.* **1969**, *40*, 761.
(23) Beaglehole, D. *Physica* **1980**, *100B*, 163.
(24) Kerker, M. *The scattering of light and other electromagnetic radiation*; Academic Press: New York, 1969.
(25) Moonen, J.; Pathmamanoharan, C.; Vrij, A. *J. Colloid Interface Sci.* **1989**, *131*, 349.
(26) Kegel, W. K. Thesis Universiteit Utrecht, 1993.
(27) Helfrich, W. In Balian, R., Kléman, M., Poirier, J. P., Eds. *Les Houches*, Session XXXV, 1980; *Physics of Defects*; North Holland, Amsterdam, 1981; p 715].
(28) Sicoli, F.; Langevin, D.; Lee, L. T. *J. Chem. Phys.* **1993**, *99*, 4759.
(29) Kellay, H.; Binks, B. P.; Hendrikx, Y.; Lee, L. T.; Meunier, M. *Adv. Colloid Interface Sci.* **1994**, *49*, 85.
(30) Guinier, A.; Fournet, G. *Small Angle Scattering of X-rays*; Wiley: New York, 1955.

JP941777F